2

KGI - PREPR -- 079

BOUNDARY LAYER PLASMAS AS A SOURCE FOR HIGH-LATITUDE, EARLY AFTERNOON, AURORAL ARCS

Rickard Lundin and David S. Evans

KGI PREPRINT 079

FEBRUARY 1985

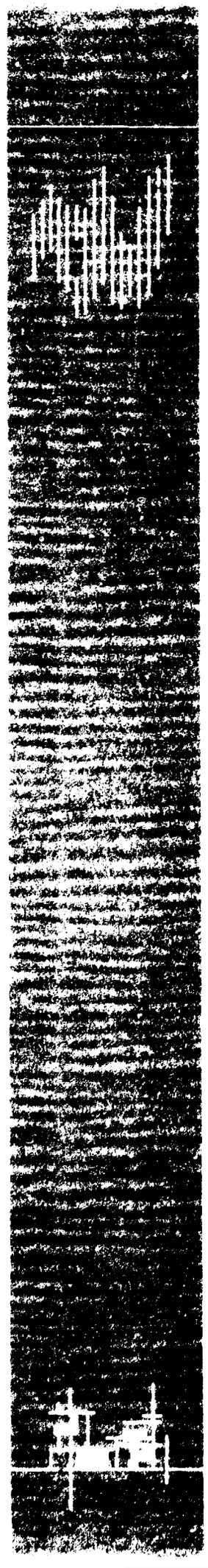

KIRUNA GEOPHYSICAL INSTITUTE
KIRUNA SWEDEN

BOUNDARY LAYER PLASMAS AS A SOURCE FOR HIGH-LATITUDE, EARLY AFTERNOON, AURORAL ARCS

by

Rickard Lundin*
The Johns Hopkins University
Applied Physics Laboratory
Laurel, Maryland 20707

David S. Evans**
Space Sciences Laboratory
Lockheed Palo Alto Research Laboratory
Palo Alto, California 94304

KGI Preprint 079
February 1985

Printed in Sweden
Kiruna Geophysical Institute
Kiruna, 1985
ISSN 0349-2656

* permanent address: Kiruna Geophysical Institute, S-981 27, Kiruna, Sweden

** permanent address: Space Environment Laboratory, Boulder, Colorado

Abstract

Simultaneous measurements of hot boundary layer plasma from PROGNOZ-7 and particle precipitation from the TIROS/NOAA satellite in nearly magnetically conjugate regions have been used to study the dynamo process responsible for the formation of high latitude, early afternoon, auroral arcs.

Characteristic for the PROGNOZ-7 observations in the dayside boundary layer at high latitudes is the frequent occurrence of regions with injected magnetosheath plasma embedded in a "halo" of antisunward flowing magnetosphere plasma. The injected magnetosheath plasma have several features which indicate that it also acts as a local source of EMF in the boundary layer. The process resembles that of a local MHD dynamo driven by the excess drift velocity of the injected magnetosheath plasma relative to the background magnetospheric plasma.

The dynamo region is capable of driving field-aligned currents that couple to the ionosphere, where the upward current is associated with the high latitude auroral arcs.

We demonstrate that the large-scale morphology as well as the detailed data intercomparison between PROGNOZ-7 and TIROS-N both agree well with a local injection of magnetosheath plasma into the dayside boundary layer as the main dynamo process powering the high-latitude, early afternoon auroral arcs.

1. Introduction

The dayside magnetopause and boundary layer have been subject to detailed studies by a number of satellite experiments during the last decade.

The high latitude portion of the dayside boundary layer near the cusp -- the "Entry Layer" -- was suggested to be the major injection region for magnetosheath plasma into the magnetosphere (e.g. Paschmann et al., 1976 and Haerendel et al., 1978). Based on the HEOS-2 results, Haerendel and Paschmann (1975) and Haerendel et al. (1978) also speculated on the energy and mass transfer of magnetosheath plasma into the polar cusp. Eastman et al. (1976) and Eastman (1979) using IMP-6 data discussed the importance of the low latitude boundary layer (LLBL) for the transfer of solar wind energy into the magnetosphere. Eastman et al. (1976) noted e.g. that the LLBL frequently contained a strong plasma drift in the direction of the magnetosheath flow, suggesting a viscous type of interaction between the magnetosphere and magnetosheath. Strongly enhanced diffusion of magnetosheath plasma through the magnetopause was believed to result in this plasma $\underline{v}\times\underline{B}$ motion. Eastman et al. (1976) also suggested that the plasma flow in the boundary layer acts as an MHD dynamo powering the large scale magnetospheric current system connected to the cusp.

The advent of high-resolution measurements from the ISEE spacecrafts have to a large extent modified our view on the structure of the magnetospheric boundary layers. Specifically, the dayside boundary layer have been found to be much more structured (e.g. Sckopke et al, 1981) and subject to stronger temporal variations than was previously believed. To a large extent the phenomenological description of the solar wind energy and momentum transfer into the magnetosphere have been based on the merging/reconnection formalism (see e.g. Paschmann et al. 1979), Sonnerup et al, 1981, Speiser and Williams,

1981, Daly et al., 1981 and Paschmann et al., 1981 for plasma data results and Russell and Elphic, 1979, Cowley et al., 1983 and Saunders, 1983 for magnetic field data results). Basically, the merging/reconnection model assumes an externally applied source of EMF (in the solar wind) which the magnetospheric plasma simply responds to. The boundary layer is according to this picture mainly a transport region for plasma on open magnetic field lines. Description of the plasma transport is simplified by assuming "ideal" MHD ("frozen-in-field" concept).

The merging/reconnection hypothesis is fundamentally different from the diffusive "viscous" interaction model suggested by Eastman et al. (1976) and the subsequent temporal dependent "impulsive penetration" model by Lemaire, 1977, 1979 and Heikkila, 1979, 1982. Although the existence of "viscous" interaction in general is acknowledged, it is often only regarded a minor supplement to the large scale convection driven by the merging/reconnection process (e.g. Cowley, 1983). On the other hand, Heikkila (1983) has demonstrated that the "viscous" interaction and the addition of structured plasma penetration, may be sufficient to explain the large scale magnetospheric dynamo processes.

Lundin and Aparicio (1982), Lundin and Dubinin (1984, a,b) and Lundin (1984) have used PROGNOZ-7 ion composition data to show that the magnetospheric boundary layers are indeed very structured and often contain regions with high β magnetosheath injection structures. The magnetosheath injection structures are associated with a $\underline{v}\times\underline{B}$ drift which is larger than observed in adjacent regions. If the $\underline{v}\times\underline{B}$ motion is interpreted as a convection, it gives a radial electric field in the boundary layer (inward at dusk and outward at dawn). These data therefore corroborate the picture of the dayside boundary layer as a generator region which through polarization of the boundary layer

sustains magnetospheric convection and drives the dayside large scale current system (e.g. Ijima and Potemra, 1978) in contrast to a convection pattern imposed externally from the solar wind. This illustrates the basic difference in view of the magnetospheric dynamo between the merging/reconnection formalism and the local boundary layer polarization model.

More recent papers by Lundin and Dubinin (1984b) and Stasiewicz et al. (1985) also clearly demonstrates that "ideal" MHD cannot be applied in the boundary layer. This is not only related to conceptual difficulties with the local field aligned conductivity ($\sigma_{\parallel} \rightarrow \infty$) but is also a consequence of simple first order drift theory applied to a plasma with strong pressure gradients and temperature anisotropies, characteristic for the boundary layer plasma. This suggests that the electric field drift may be much smaller than other characteristic drifts of the plasma (due to e.g. the plasma inertia, pressure gradients and perpendicular currents). For these reasons the electric field inferred from the $\underline{v}\times\underline{B}$ motion of the plasma may differ substantially from the actual local electric field sensed by the plasma.

Ijima and Potemra (1978) found that the Region 1 field aligned currents (FAC) exhibited two maxima versus local time -- an upward FAC maximum in the 14-16 MLT sector and a downward FAC maximum in the 8-10 MLT sector. Bythrow et al. (1981) concluded that these Region 1 current maxima are coincident with the dayside high latitude extension of the low-latitude boundary layer (LLBL). Optical studies from the ISIS-2 satellite (Murphree et al., 1981) also revealed the existence of "isolated arcs" in the early afternoon sector, controlled by the interplanetary magnetic field (IMF) By-component. The fact that these early afternoon arcs at times appear to be "isolated" from the evening/nightside auroral arcs, and to some extent occur independent of the general auroral activity on the nightside, led Akasofu and Kan (1980) to

believe that the dayside auroral oval is not a natural extension of the nightside one. Akasofu (1981) also argued that, on phenomenological grounds, the aurora along the oval can be separated in three different categories:

1. The dayside discrete aurora.
2. The nightside discrete aurora, and
3. the diffuse aurora, which is not local time dependent.

Recently Evans (1984) also reported about the persistency of the "isolated" auroral arcs at high latitudes in the 1400 MLT sector. Moreover, he also showed that the auroral structures were latitudinally very thin and composed entirely of precipitating 0.3-3 keV electrons originating from a source plasma of comparatively high densities (≈ 2 cm^3) and low temperatures ($\approx$150 eV). Parallel electric field acceleration through $\approx$1000 V potential difference appeared to be responsible for the electron energy flux enhancements in the auroral structures. An important characteristic of the 1400 MLT auroral arcs is also that they may comprise several parallel arc structures distributed within some five degrees in latitude. This suggests that the corresponding dynamo region in the outer magnetosphere may be strongly filamentary. The topological shape of this filamentation will be one in a series of arguments for the dayside LLBL as the site of the dynamo process responsible for the EMF driving the region 1 FAC's and resulting in the discrete aurora around 1400. Evans (1984) also argued that the low temperature and relatively high density suggested a source plasma of injected magnetosheath electrons. Robinson et al. (1984) found from incoherent scatter data that the persistent density enhancement in the F-region, which occurred in the $\approx$1400 MLT local time sector, was associated with a reversal in the plasma convection. The convection geometry is much the same as that found in the evening/nightside part of the oval in e.g. "inverted V" events (Frank and

Gurnett, 1972). The process responsible for downward acceleration and precipitation of electrons in the "isolated" 1400 MLT arcs is thus similar to that in the evening/nightside sector associated with discrete "inverted V" type of auroral arcs -- yet the dynamo regions may be topologically separated. In this study we will present a quite unique set of data taken simultaneously in the high latitude auroral region (TIROS-N) as well as directly in the nearly conjugate LLBL - dynamo region (PROGNOZ-7). The data does not only show a remarkable topological similarity in terms of boundary characteristics, but it also provides a surprisingly good agreement between measured and inferred source plasma parameters and the expected dynamo signature responsible for the ≈1400 MLT electron acceleration and precipitation.

This favorable comparison occurred for the only instance of proper satellite positioning that we currently have available to us.

Observations Made by the TIROS/N and PROGNOZ-7 Satellites

The TIROS-N satellite, a meteorological spacecraft in sun-synchronous, near circular orbit (98° inclination, 850 km altitude), had a charged particle instrument which measured precipitating charged particles in the energy range 0.3 - >100 keV. The instrument comprised swept electrostatic analyzers (0.3-20 keV) and solid state detectors (>30 keV) for both ions and electrons. For a more comprehensive description of the experiment the reader is referred to Evans (1984).

Figure 1 shows the highest time resolution (2 second) observations of the precipitating electron energy flux and characteristic electron energy (uppermost two panels), >30 keV electrons with 90° pitch angle and >30 keV positive ions with 90° pitch angle. The electron energy flux and

characteristic energy (= the energy band containing the maximum in the differential energy flux) was obtained by on board processing of the data. Notice that the time axis has been reversed (for intercomparison reasons that will become obvious in Figure 2). The energy flux panel shows two flux enhancements (13.7 erg/cm^2 s and 0.95 erg/cm^2 s) at ≈73.5° and ≈72.7° invariant latitude. These flux enhancements are related to the thin ($\lesssim$16 km) auroral arc structures in the ≈13 - 14 MLT sector. Both arc structures are embedded within very low energetic electron fluxes poleward of what appears to be a boundary for energetic electrons. The poleward arc also coincides with what appears to be a boundary for energetic ions. The location of discrete aurora on, or poleward of, a region of stably trapped particles was recognized already in the early seventies (e.g. Frank and Ackerson, 1971, Winningham et al., 1975). The implication of this boundary in the nightside plasma sheet was discussed by Winningham et al. (1975) who also introduced the distinction between the "central plasma sheet" and "boundary plasma sheet" to substorm process. Moreover, Eastman et al. (1984) argued that the "plasma sheet boundary layer" is a persistent feature of the plasma sheet associated with e.g. auroral acceleration processes. Lyons and Evans (1984) using TIROS-N data from the evening sector showed that discrete auroral precipitation is often coincident with plasma boundaries and suggested that these boundaries may, in turn, often be associated with structures in the plasma sheet outer boundary which act as dynamos which drive the auroral acceleration process.

The dayside auroral region pass shown in Figure 1 is thus in many respects similar to those made on the evening/nightside, except that the boundary is here related to the dayside LLBL. Figure 2 shows PROGNOZ-7 plasma data taken during an inbound pass of the high latitude part of the LLBL (≈48° GSM latitude). The local time of the pass is 15.5 (GSM). Considering the

tailward field line draping, this probably traces very close to the magnetic local time of the TIROS-N pass. The uppermost total plasma density panel displays one distinctive density enhancement (≈2.8 cm^{-3}) and two minor enhancements (≈1.0 and 0.8 cm^{-3} at ≈08.53, 08:59 and 09:01 respectively. The second and third panel shows the partial ion and electron densities above 7 and 11 keV, respectively. The fourth panel shows the electron temperature and the two bottom panels depict the electric field (in solar ecliptic coordinates) inferred from the ion $\underline{v}\times\underline{B}$ motion of the proton-dominated boundary layer plasma. Only the εx (sunward) and εy (duskward) components are shown here. As have been demonstrated by Lundin and Dubinin (1984 a,b), Lundin (1984) and Stasiewicz et al. (1985) the boundary layer electric field is not uniquely determined by the plasma $\underline{v}\times\underline{B}$ motion, so great caution should be assessed when relating $\underline{\varepsilon}$ and $\underline{v}\times\underline{B}$.

The PROGNOZ-7 data in Figure 2 was collected when the instrument operated in a high data rate mode which enabled moments of the plasma distribution function to be obtained within one satellite spin (≈2 minutes). The ion composition experiment, described in more detail by Lundin et al. (1982), provided reasonably accurate flow vectors whenever the flow had a strong YZ or -X (antisunward) flow component. The latter is usually the case in the dayside boundary layers. These flow vectors were then used to determine the $\underline{v}\times\underline{B}$ motion in the lower panel.

Notice that Figure 2 represents the innermost part of the boundary layer. The first magnetopause encounter occurred some 1.5 hour prior to this (at ≈07.25 UT). However, the experiment was then working in a low bit rate mode unsuitable for this kind of study.

Although temporal variations are supposedly very important in the boundary layer, we will assume for the PROGNOZ-7-TIROS-N comparison that very

limited temporal/spatial variations occurred within the approximately ten minutes of detailed intercomparison. Moreover, we assume that the spatial configuration of the LLBL is reasonably well represented by the PROGNOZ-7 radial crossing. We then find the following similarities between the two passes:

The largest total particle density enhancement is located immediately outside of the region of generally increasing density of >11 keV electrons. The other small enhancements in total number density are associated with local decreases in the density of electrons >11 keV. The auroral structures passed by TIROS-N shows similar topological features in the >30 keV electron fluxes.

There is a local decrease in the density of >7 keV ions coincident with the total number density enhancements seen at PROGNOZ-7 and, in addition, the energetic ion particle density is somewhat lower in the region of the total density enhancement than radially inside of it. Although less dramatic, this variation at PROGNOZ-7 replicates the large variation in >30 keV proton fluxes seen at low altitude coincident with the most intense arc. Overall the much more pronounced boundary characteristics on the low altitude measurement is probably related to the difference in energy range covered (8-30 keV and >30 keV). The temperature panel in Figure 2 shows that the electron temperature remained fairly constant throughout this pass. Only in the innermost part did a slight increase from ≈100 eV to ≈130 eV occur. The ions, however, showed very strong temperature fluctuations, the temperature varying from ~800 eV inside the high density structures to ~7 keV outside (e.g. Lundin and Dubinin, 1984, their Figure 3).

The $\underline{v}\times\underline{B}$ motion of the boundary layer plasma adds conclusive information about the dynamo related auroral electron acceleration and precipitation measured from the low altitude TIROS-N spacecraft. Both the ≈08:53 and 08:59

UT enhancements are characterized by drift reversals -- indicating a negative space charging at the center ($\underline{\nabla} \cdot \underline{E} < 0$). This should not only require neutralizing currents to flow into this region but may also lead to the development of auroral arcs (Lyons, 1980, 1981, Chui and Cornwall, 1980). Thus, we may expect the density enhancement and drift reversal to be associated with both an upward current and an auroral arc.

In the following sections we will make a quantitative intercomparison between the PROGNOZ-7 and TIROS-N data and put that in the frame of the auroral dynamo model.

3. Quantitative TIROS-N and PROGNOZ-7 Intercomparison

Evans (1974) demonstrated that the electron fluxes just above auroral arcs are often reasonably well represented by a "primary" Maxwellian source distribution (density n_o and temperature E_o) accelerated through a magnetic field aligned potential V_o, and a "secondary" atmospheric backscattered electron distribution. Together they form the typically peaked auroral electron spectrum (e.g. Evans, 1969 and Frank and Ackerson, 1971).

The energy input is determined by the "primary" electron source density and temperature and the accelerating voltage magnitude and altitude above the atmosphere. An expression for this energy input was derived by Lundin and Sandahl (1978). If the accelerating potential is located sufficiently high up ($B_a >> B_i$, see e.g. Lundin and Sandahl, 1978) we may write for the energy flux of the precipitating electrons:

$$F = 5.36 \times 10^{-5} \frac{n_o}{E_o^{1/2}} \left[V_o^2 + 2E_o V_o + 2E_o^2 \right] \ (\mathrm{erg/cm^2 s})$$

where n_o is the density in cm^{-3}, E_o the temperature in eV and V_o the accelerating voltage. Notice also that for $E_o << V_o$ we get $F \approx 5.36 \times 10^{-5} n_o V_o^2 / E_o^{1/2}$, an expression which reasonably well follows experimental data (e.g. Lundin and Sandahl, 1978 and Lyons et al., 1979).

From the TIROS-N data we use the two highest energy flux structures at 08:58:49 UT and 08:58:35 UT (13.7 erg/cm^2 s and 0.95 erg/cm^2 s respectively). The "characteristic energy", corresponding to the energy of maximum flux, were 930 eV and 380 eV respectively for these structures. For an accelerated Maxwellian the "characteristic energy" should correspond closely to the accelerating voltage (V_o) if $E_o < V_o$. Notice that 380 eV is the lowest energy channel of the TIROS-N instrument. The accelerating voltage may therefore have been less than 380 eV, even for $E_o > V_o$. Thus, we have chosen the somewhat lower value of 300 V for V_o in the latter case. The lack of direct TIROS-N temperature measurements for this specific pass means that we have to rely on the PROGNOZ-7 temperature measurements. However, typically the source electron temperatures in the 1400 MLT arcs average ≈150 eV, very close to the ≈100 eV PROGNOZ-7 observation in this case (see Evans, 1984). By using the PROGNOZ-7 electron temperature and values of F and V_o from the low altitude data, in Equation 1 we get the density of the precipitating electrons. The result for the two cases we have discussed is shown in Table 1. Clearly Table 1 shows that the densities for the precipitating electrons are similar to the densities in the PROGNOZ-7 enhancements at 08:53 UT and 08:59 UT.

This suggests that auroral structures identified by TIROS-N in the 1400 MLT sector are related to density enhancements in the dayside boundary layer.

According to Lundin and Dubinin (1984a), these density enhancements are a result of magnetosheath plasma being injected into the dayside boundary layer.

The excess momentum of the injected plasma represents a source of free energy that is converted into electromagnetic energy (electric field) -- i.e. the "injection structures" acts as local MHD-generators (Lundin, 1984 and Lundin and Dubinin, 1984b).

In a simple MHD model, the maximum potential available to the region of space external to the dynamo is the line integral of the motionally induced electric field, $\underline{v}\times\underline{B}$, across the dimension of the dynamo where $\underline{v}$ is the velocity of the injected plasma relative to the earth. This line integration may be performed using the PROGNOZ-7 observations of the bulk flow velocity of the injected plasma to deduce the motionally induced electric field and presuming that the satellite traversed the appropriate dynamo region from one side to the other. Using PROGNOZ-7 observations between 0848 and 0854 UT, spanning the number density enhancement at 0853 and associated electric field reversal, we obtain a total potential difference of 1200 ± 100 V. A similar integration using data spanning the density enhancement at 0859 UT yields a potential difference of 900 ± 100V. In both cases the motionally induced electric field appropriate to these potential differences is in the radial direction.

In Table 1 we compare the magnitudes of the available induced potential across the two density enhancements with the field-aligned potentials inferred from the TIROS-N electron measurements over the two precipitation regions that we identify with these instances of high altitude, injected plasma. In both cases the inferred field-aligned potentials are of order or less than the estimate of the available motionally induced EMF.

If an energy transfer from the kinetic energy of the bulk motion of the injected plasma to the ionosphere (accelerated precipitating electrons and Joule dissipation) is occurring by virtue of a current system threading both

the ionosphere and dynamo by means of field-aligned currents, we expect that the actual available potential is somewhat less than the maximum we have estimated. This is to say that if the dynamo is under load, then by necessity the motionally induced electric field is not entirely balanced by a local electric field associated with charge separation so that $\underline{\varepsilon}+\underline{v}\times\underline{B}$ no longer equals zero. In such a situation a line integration of $\underline{\varepsilon}$ across the dynamo region provides the magnitude of the potential available from the loaded dynamo, and that potential ought to be compared to the potentials inferred to exist in the circuit external to the dynamo from the TIROS-N measurements.

Lundin (1984) and Lundin and Dubinin (1984b) have argued that the PROGNOZ-7 observations of the bulk motion of "local plasma" (e.g. O^+ or He^+ which have originated from the ionosphere) provides a measure of the local electric field, $\underline{\varepsilon}$, which is traced to charge separation across the dynamo. Using the bulk flows observed in O^+ while PROGNOZ-7 transited the density enhancements we have line integrated $\underline{\varepsilon}$ in the same manner as the line integration of the motionally induced electric field $\underline{v}\times\underline{B}$ to obtain the potentials V_l listed also in Table 1. These potentials V_l are less than the potentials inferred to exist along the magnetic field from the TIROS-N data. We ascribe this disagreement to inadequate knowledge of the geometry over which to perform these line integrals, to the ambiguities introduced by possible proper motion of the dynamo region relative to the earth, to temporal variations, or to a combination of these effects none of which can be resolved by a single satellite. Of these effects, the first is likely the most important. When $\underline{\varepsilon}+\underline{v}\times\underline{B}$ is not zero, $\underline{\varepsilon}$ is not simply different in magnitude from $\underline{v}\times\underline{B}$ but will differ in direction as well and, indeed, need not even be in a direction normal to $\underline{B}$ (i.e. it may have a component along $\underline{B}$). Thus the appropriate line integration along $\underline{\varepsilon}$ is not only different than the

appropriate line integration of $\underline{v} \times \underline{B}$, but may also require a portion of the integration path to lay along $\underline{B}$ introducing a third dimension to the problem which even two satellites would be unable to resolve. We regard this as being the primary reason for an underestimate of the available potential from the loaded dynamo situation that is applicable to the PROGNOZ-7/NOAA-6 comparison.

In summary, this TIROS-N and PROGNOZ-7 case study have demonstrated a remarkable similarity between the plasma characteristics in the dayside LLBL and the particle precipitation in the high latitude auroral ionosphere near 1400 MLT. We have identified the magnetosheath injection structures (Lundin and Dubinin, 1984a) in the boundary layer as a source of EMF, driving a local current circuit and responsible for the acceleration of electrons associated with the ≈1400 arc structures. The process is similar to that first suggested by Eastman et al. (1976), only with the difference that local magnetosheath injection structures provides a more massive plasma entry as well as a strong filamentation of the boundary layer with respect to plasma, fields and currents. The "image" of this filamentation in the boundary layer is the multiple arc structure observed at low altitude. In the following sections, we will address the characteristics of the plasma filamentation in the boundary layer -- topologically as well as with respect to currents and fields.

4. Plasma Penetration - Large Scale Morphology

The first to consider a process for structured injection of magnetosheath plasma into the dayside boundary layer was Lemaire (1977). Later Lemaire et al. (1979) and Heikkila (1979, 1982a, b) discussed the "impulsive penetration" process from various "conditional" points of views (IMF-dependence and local plasma parameters sustaining the plasma entry). Despite these theoretical investigations, a fully recognized theory for plasma penetration through the

magnetopause is yet to be developed. However, we have now quite firm experimental evidences for that plasma may penetrate the magnetopause and form "blobs" of high density, high β magnetosheath-like structures in the magnetospheric boundary layers (e.g. Sckopke et al., 1981, Lundin and Aparicio, 1982 and Lundin et al., 1983).

Sckopke et al. (1981) presented a morphological picture with "blobs" of magnetosheath plasma sliding along the magnetopause surface. The drift of these "blobs" were believed to be controlled by a combination of a "viscous" interaction with the magnetosheath flow and the internal plasma convection -- with vortex-motions of the plasma in the "blobs" related to a Kelvin-Helmholz instability. Cowley et al. (1983) later discussed these "blobs" in the frame of flux transfer events -- the plasma drift in the boundary layer resulting from the "drag" of open field lines driven by the electrically-connected external plasma flow. Notice that the plasma in these models is assumed to simply respond to an externally applied electric and an ambient magnetic field without the plasma modifying these fields.

A somewhat different view on what is supposed to be quite similar observations, but measured on another spacecraft, was presented by Lundin (1984) and Lundin and Dubinin (1984b). Here the plasma drift is believed to cause, or at least strongly perturb, the ambient fields. Electric fields result from plasma polarization, and magnetic perturbations are caused by local currents. The model is basically the well known MHD-generator driven by an excess plasma momentum (see e.g. Rostoker and Bostrom, 1976). The large scale morphology -- in terms of currents and fields -- of this model have been discussed by Heikkila (1979, 1984). Figure 3 shows a near ecliptic plane projection of the plasma flow (open arrows) and currents (solid arrows) that results from a boundary layer dynamo driven by magnetosheath plasma

penetration. The field aligned currents driven by the LLBL dynamo, upward in the early afternoon and downward in the late morning, agrees with experimental findings of the dayside Region 1 currents (e.g. Ijima and Potemra, 1978). Current closure is maintained by the dayside auroral oval ionosphere (Pedersen/Hall currents) and by a magnetopause current (marked jMP). The magnetopause current system is likely to have a strong out of plane orientation. This is indicated by the dashed lines connected to the magnetopause in Figure 3.

Notice also that the LLBL is expected to be mapped on a limited, crescent shaped, part of the dayside ionosphere close to the cusp (see e.g. Vasyliunas, 1979). Auroral phenomena related to the LLBL is thus confined to a limited local time sector in the dayside (e.g. 0800-1600 MLT). This illustrates the strong distinction between dayside and nightside auroral phenomena, pointed out by e.g. Akasofu (1981). We may already conclude, on the basis of what we know of current directions and discrete aurora, that the discrete aurora have a preference for the duskside (upward currents) in this model (i.e. between 1200 and 1600 MLT). Notice, however, that the connection between discrete aurora-caused by downward acceleration of electrons and upward currents should be interpreted as a space-charge phenomena instead of a current induced phenomena (e.g. Lennartson, 1977). The magnetic mirroring will be a sufficient reason for maintaining a parallel potential drop between the ionosphere and the negatively charged side of the LLBL dynamo.

The lower part of Figure 3 shows an enlarged part of the evening LLBL dynamo. The perpendicular current ($j_\perp$) in the LLBL is the polarization current driven by the plasma flow ($\underline{v}$) perpendicular to the ambient magnetic field ($\underline{B}_m$), and maintained by the replenishment of charges by current flow along the field lines connecting the ionosphere.

Notice that $\underline{j}_\perp \cdot \underline{\varepsilon}_\perp < 0$, as it should be in a dynamo, and that the electric field in the frame of reference of the moving plasma ($\varepsilon_\perp^*$) is nonzero. $\varepsilon_\perp^* < 0$ indicates that the dynamo plasma sees an electric field in its own frame of reference which is opposite to the polarization field -- that is, it experiences a braking force. This is the force which extracts energy from the plasma and drives the current. For further details about the dynamo model, see e.g. Lundin and Dubinin (1984b).

A particular feature of the return current on the magnetosheath-side of the magnetopause is that it has a component along the field lines. We believe that this is the distinguishing characteristics of what is called flux transfer events (the magnetic perturbation of field aligned current tubes connected to "blobs" of plasma penetration).

Figure 3 demonstrates how the overall current and field characteristics of the LLBL dynamo model agrees with the statistical results from low-altitude measurements (e.g. Ijima and Potemra, 1978, Bythrow et al., 1981 and Evans, 1984).

A consequence of the polarization model proposed in Figure 3 is that the electric field in the boundary layer should point inward at dusk and outward at dawn (see Heikkila, 1979). This orientation was also confirmed by Lundin and Dubinin (1984a, b) from dayside passes of the boundary layer at high latitudes near noon and by Eastman et al. (1976) and Eastman (1979) within the low-latitude boundary layer farther from local noon.

Figures 4 and 5 show two examples of Prognoz-7 boundary layer crossings which illustrates this polarization effect. Figure 4 represents the 3 January 1979 case with TIROS-N data. The upper panel gives ion densities (in a linear scale) and the lower panel the relative potential along the satellite trajectory. In Figure 4 the relative potential is referred to 08:42 UT (see Figure 2) while in Figure 5 it is referred to the time of the magnetopause

crossing (03:19 UT, see e.g. Lundin and Dubinin, 1984a). The relative potential was deduced by accumulating the product of $\underline{v}\times\underline{B}$ and $\underline{s}$ (distance along the satellite trajectory) for H^+, O^+ and E/q ion data. For the E/q ion data, we assumed all ions were protons. Figure 4 shows how the "motional" EMF ($\Delta\phi$) across the high density ($\approx$2.7 cm^3) injection structure was inferred. The electrostatic analyzer (E/q) data was preferred here because of a more complete energy coverage ($\approx$0.03-30 keV/e) as compared to the ion composition spectrometers (0.2-17 keV/e). However, the assumption is then that all ions are protons, an assumption that is basically only appropriate in the injection structures.

Figure 4 displays two important characteristics of this dusk boundary layer pass. The first is the negative polarization of the inner edge, in agreement with the polarization pictured in Figure 3. The essentially radial cross section of the boundary layer (imposed by the Prognoz-7 trajectory) thus suggests a radially oriented "motional EMF" of at least 10 kV over this orbit element. Notice that the H^+ and E/q (assuming protons) relative potential agrees reasonably well. The somewhat lower E/q voltage may have resulted from the presence of heavy ion fluxes. The second important characteristics is that the O^+ ions only provided a drop in relative potential (along the limited part of the satellite trajectory) of about -1 kV as compared to $\sim$-11 kV for the H^+ ions. Although some of the discrepancy between the H^+ and O^+ potential distribution may be attributed to cumulative measurement errors, the major reason for this discrepancy must be related to a local difference in the electrostatic potential distribution and the "motional" EMF. Such differences are consistent with a dynamo under load -- the larger the difference, the higher the rate of energy transfer. An additional reason for this difference is that polarization occurs along the field lines as well. Thus we have not

with the present integration path (almost perpendicular to B) succeeded to integrate over $\underline{\varepsilon}$, only over $\underline{v \times B}$ in the dynamo. The difference between relative potentials for H^+ and O^+ in Figure 4 may therefore also be due to the presence of electrostatic potentials along the field line. Figure 5 shows the potential distribution along the PROGNOZ-7 trajectory for a dawn boundary layer pass (9 February 1979, see e.g. Lundin and Dubinin, 1984a). The relative potential is now taken from the magnetopause and inward. Notice first of all that the polarization is increasingly positive inward, as compared to increasingly negative in the previous dusk case. Again, this confirms the polarization picture proposed in Figure 3.

During this boundary layer pass, the satellite encountered three high density magnetosheath injection structures. All three injection structures were associated with a considerably increased polarization potential which also could precede the density enhancement. Apparently the polarization is enhanced by the injection structures. Notice for instance that the relative potential has an inflection point, or even a small minima, after passing the structure. We interpret this as an inward motion of the potential (injection) structure -- briefly encountering the negatively polarized side of it. The topology of this will become apparent in the next two sections. Since the negatively polarized side should be connected with an upward current and possibly a field-aligned potential drop, we expect this to be associated with a discrete auroral structure in the pre-noon sector. Unfortunately, no TIROS-N pass was suitable for a near-simultaneous intercomparison with this PROGNOZ-7 pass. However the two passes around the time of the PROGNOZ-7 magnetopause crossing showed quite strong (5-15 erg/cm^{2}s) narrow arc structures located in the pre-noon sector, as one would expect from the PROGNOZ-7 data.

Except for the sign of the polarization, another important difference between the dawn and dusk pass (Figures 4 and 5) is the relative potential given by the O^+ ions. Evidently the difference between the local plasma drift (= convection) and the injected plasma drift (= the dynamo) was much smaller at dawn. A viable interpretation of this is that the dynamo now is not nearly as "heavily" loaded as it was in the previous dusk sector pass. A contributing factor for the smaller difference between the H^+ and O^+ relative potentials is also that the field lines in the morningside, dominated by downward currents, are more equipotential-like.

5. Plasma Injection Filaments and Multiple Arcs

Evans (1984) demonstrated that the dayside ≈1400 MLT precipitation usually consists of multiple structures, at times distributed over a considerable latitude interval ($\gtrsim 5°$). DMSP pictures (Meng, private communication, 1984) also show a striation of these arcs in a way previously suggested by Akasofu (1981).

Figure 6 attempts to demonstrate the relation between individual injection filaments and discrete auroral arc structures.

The upper part of Figure 6 shows how the negatively charged side of each plasma injection filament results in an upward current sheet which connects along one specific auroral arc structure. The bottom part of Figure 6 gives an enlarged top view of the auroral oval with discrete auroral structures embedded in a "background" of diffuse aurora. We emphasize here the "radial" dependence of the discrete aurora on the dayside. The radial striation (see e.g. Akasofu, 1984) should have an apparent focusing towards the polar cusp. This reflects the site of plasma injection in the dayside boundary layer -- the "entry layer". We have used a wider definition of the "entry layer" than that used by e.g. Paschmann et al. (1976). The "entry layer" may here also include the LLBL near the subsolar point. Topologically, however, it is

difficult to distinguish between LLBL and the "entry layer" near noon, since they may both connect to the polar cusp.

The length of the individual arc structures reflect the extension of the plasma injection structures in the boundary layer. Typically multiple dayside arc structures extends 1-3 hours MLT along the auroral oval (Meng, private communication). This corresponds to a length of 3-9 R_E of the injection structures in the boundary layer using a dipole magnetic field projection. On the other hand, the substantial tailward distorsion of the magnetic field at the outer boundary of the LLBL suggests that even a limited radial cutting across flux tubes may give rise to an ionospheric footprint similar to that proposed in Figure 6 (eg Eastman et al.,1976).

Considering the plasma injection as a temporal process -- the plasma traversing magnetic field lines as a result of its excess momentum -- Lundin (1984) showed that a plausible lifetime for such a process is of the order a few minutes (for an entirely perpendicular expansion). This lifetime depends on among other things the conductivity in the load (the ionosphere) and the mass-density of the injected plasma. Other important factors for the "slowing down" (=energy transfer) time is the length of the flux tube which relates to the time for the ionosphere to respond to the dynamo process. The latter may increase the length of the spatial injection structure in the boundary layer considerably. Based on a lifetime of a few minutes and an initial drift velocity ranging from 100-300 km/s in the boundary layer, the injection structure should expand a few R_E perpendicular to the magnetic field before being stopped. As a result of the "field line draping" in the boundary layer, the projected length of the perpendicular expansion in the boundary layer will be considerably longer. Eventually, the injected plasma have lost all its excess momentum perpendicular to $\underline{B}$. The boundary layer plasma motion is then entirely controlled by the ambient fields ($\underline{\varepsilon}$ and $\underline{B}$) and the flow is predominantly field aligned (flank/tail LLBL).

Notice that the topological model of Figure 6 predicts that discrete arc structures may appear in the late morning as well. However, they will only be related to the inside/dawnside part of the injection filaments where a negative charge may build up. Thus, unless a very deep penetration and strong filamentation occurs, the late morning discrete auroral structures are expected to have a very limited local time extension.

In conclusion, the plasma injection model described in Figure 6 can account for many topological characteristics of the dayside discrete aurora, such as multiple arcs and their "radial" dependence.

Finally, we will attempt to relate the topology of a plasma injection element to the act al measurements on PROGNOZ-7.

Figure 7 shows a series of panels which illustrate the plausible temporal development of a boundary layer injection element inside the early afternoon magnetopause. The shaded area corresponds to the region of enhanced plasma density expanding inward and tailward in the boundary layer. As in Figure 3, the magnetic field Z-component is here directed out of the plane of this ecliptic XY-projection. The negatively charged side of the plasma filament will drive the upward Birkeland current sheet associated with the field-aligned acceleration process. Notice that we have included a "partial" return current to the ionosphere on the positively charged side of the filament.

The six panels in Figure 7 are related to the periods indicated in Figure 2. The spacecraft position is given by the locus of the $\underline{\varepsilon}$ and $\Delta\underline{B}$ vectors in each panel. As in Figure 2, the magnitude and orientation of the $\underline{\varepsilon}$ vector is obtained from the plasma $\underline{v}\times\underline{B}$ motion which may be different than the electric field as noted in Section 3 above. As for the $\Delta\underline{B}$ vector, it was deduced from the inferred perturbation of Bx and By along the orbit of the spacecraft (see e.g. Figure 3 in Lundin and Dubinin, 1984a). Furthermore, this perturbation was

believed to be due to field aligned currents outside the structure and a combined field aligned and perpendicular current inside the injection structure.

Notice from Panel 1 and 2 that $\Delta\underline{B}$ agrees quite well with the perturbation expected from a return current (downward field aligned current) on the positively charged part of the injection structure. Inside the structure, $\Delta\underline{B}$ suggests the existence of a transverse current ($j_\perp$) that is oppositely directed to the electric field inferred from the plasma $\underline{v}\times\underline{B}$ motion as well as that expected from the polarization model.

Thus, the magnetic perturbation and plasma $\underline{v}\times\underline{B}$ motion both corroborates the dynamo characteristics ($j_\perp \cdot \varepsilon_\perp < 0$) on the magnetosheath injection structure from this PROGNOZ-7 boundary layer pass. Moreover, we may conclude, from the direction of the transverse electric field (inferred from the plasma $\underline{v}\times\underline{B}$ motion, see Figures 4 and 5), that the boundary layer is being polarized in the way predicted by the plasma injection model. An alternative explanation for $\Delta\underline{B}$ is that field-aligned currents flows at the boundaries of the injection structure as Figure 7 also suggests. In fact both the transverse and field-aligned current component will cause a magnetic perturbation in the same direction for a closed current "loop". However, if at all existing, the transverse current must have the direction indicated in Figure 7.

6. Summary and Conclusions

Discrete aurora have long been known to be associated with a high altitude acceleration process that accelerates electrons downward and positive ions upward. Despite some controversy about this particular acceleration process throughout the last 15 years, the experimental evidences in favor for a quasi-electrostatic acceleration are now overwhelming. The magnetospheric

dynamo sustaining this acceleration process have been subject to speculations by e.g. Bostrom (1975), Falthammar (1978), Lennartsson (1980), Lyons (1980, 1981), Chiu and Cornwall (1980), Sonnerup (1980), Block (1984) and Stasiewicz (1984). Experimental evidences for an MHD-dynamo localized in the dayside boundary layer was first presented by Lundin and Dubinin (1984a) and Lundin (1984). Such a dynamo, driven by direct injection of magnetosheath plasma into the dayside boundary layer, was first proposed by Eastman et al. (1976), Lemaire (1977) and Heikkila (1979). The latter authors actually proposed a more massive entry of magnetosheath plasma into the boundary layer, that may account for the large scale convection as well as the magnetospheric current system. Based on the general characteristics of a region with discrete aurora in the ≈1300-1500 MLT sector (Evans, 1984 and Robinson et al., 1984) and the direct measurement of simultaneous particle data from TIROS-N and PROGNOZ-7 on nearly magnetically conjugate regions, around ≈1400 MLT, we have related the dayside boundary layer dynamo signature with the low altitude characteristics of precipitating particles. Our particle data, summarized for the two arc structures in Table 1, shows good agreement between the measured source plasma parameters in two injection filaments (PROGNOZ-7) and the plasma parameters inferred from below the acceleration region (TIROS-N). Both satellites also show that the discrete aurora/injection structures are located on a boundary for energetic electrons and ions, with the higher fluxes present magnetically equatorward.

We have also interpreted the $\underline{v}\times\underline{B}$ motion of the boundary layer plasma and concluded that the "motional" dynamo EMF is sufficient to sustain the field aligned potential drop inferred from the low-altitude measurements. Moreover, the $\underline{v}\times\underline{B}$ motion shows the expected shear characteristics from a negative polarization in the injection elements ($\nabla\cdot\underline{E}<0$). Thus the detailed comparison

of data between TIROS-N and PROGNOZ-7 have demonstrated that the dayside/flank boundary layer may act as a source of EMF for the early afternoon discrete aurora at high latitudes. Furthermore, we noted that the difference between the local potential distribution (inferred from the O^+ drift) and the "motional" EMF (inferred from the injected solar wind ion drift) is consistent with a dynamo under load. The larger this difference is - the more heavily loaded is the dynamo.

An important and conclusive characteristic of the activity near noon -- manifested by the ≈14 MLT discrete aurora (Evans, 1984) and the Region 1 current enhancement (Ijima and Potemra, 1978) -- is its persistence, even during low disturbance levels. This suggests that the dayside boundary layer process, responsible for the EMF and driving the dayside Region 1 current system, occurs independent of the nightside substorm activity and may be less sensitive to the IMF orientation. A penetration of plasma in the vicinity of the polar cusp region is in agreement with that conclusion. Once injected, the plasma may expand into what topologically corresponds to the dayside auroral oval. This should cause the "striation" of the dayside discrete aurora and the radial dependence of these arcs (see e.g. Figure 6) the proximity focused onto the polar cusp. Multiple arcs is thus the result of several plasma injections in various parts off the "center" of the cusp. However, eventually an injected plasma "cloud" may also break up into several filaments as suggested for the nightside plasma injection (Stasiewicz, 1984). Each plasma injection filament does in this model represent an individual dynamo circuit driving an upward Birkeland current sheet on the negatively charged side and a downward current sheet on the positive side. The polarization of the filament is maintained by the inertia current driven by the plasma expansion across the ambient magnetic field. The large scale/average current circuit, which depends on the average mass flow in the

boundary layer, should be downward in the ~0900-1100 MLT sector and upward in the 1300-1500 MLT sector as Figure 3 shows.

Figure 8 summarizes the plasma and field characteristics of plasma injection structures in the early afternoon sector. We have also assumed that one injection structure has expanded much more inward -- thereby providing two current circuits. The innermost current circuit is here believed to be self-contained, closing in the ionosphere by a Pedersen current and in the dynamo by the inertia current. The outermost circuit represents the quasi steady-state current circuit described by Ijima and Potemra (1978). This circuit will close in the ionosphere via a Hall/Pedersen current and at the magnetopause by the Chapman-Ferraro current connecting dawn and dusk. In Figure 8, we have indicated that the latter current may also be a field aligned magnetosheath current connecting to the solar wind (flux transfer events).

Notice that a substantial fraction of the available dynamo EMF may be distributed externally along the field lines connected to the negatively charged side. The reason for this is simply the current limitation that this part of the circuit is subject to (see e.g. Knight, 1973, Lennartsson, 1977, 1980 and Lyons, 1980). The positively charged side is not subject to the same current limitation since the downward current can be carried by upflowing ionospheric electrons.

The field aligned potential drop on the negative side will accelerate electrons downward and cause the high latitude dayside discrete aurora. Finally, we can see from the polarization pattern that the injection structures will sustain a sunward flow earthward of the negative polarization. A massive injection of plasma into the LLBL is thus capable of driving the large scale magnetospheric convection, as suggested by Heikkila (1979, 1983) and Eastman (1976).

Acknowledgement

This paper was completed when both of us were on leave from our regular positions in Kiruna and Boulder. We acknowledge the good support and hospitality shown to us at APL and Lockheed, respectively, that made our visits both pleasant and productive.

References

Akasofu, S.-I., and J.R. Kan, Dayside and nightside auroral arc systems, Geophys. Res. Lett., 7, 753, 1980.

Akasofu, S.-I., Auroral arcs and auroral potential structure, Physics of auroral arc formation, AGU, Geophysical Monograph, 26, 1981.

Block, L., Three-dimensional potential structure associated with Birkeland currents, Magnetospheric currents, AGU, Geophysical Monograph, 28, 315, 1984.

Bostrom, R., Mechanisms for driving Birkeland currents, Physics of hot plasma in the magnetosphere, (ed. Hultqvist and Stenflo), Plenum Press, New York, 1975.

Bythrow, P., R. A. Heelis, W.B. Hanson, R.A. Power, and R.A. Hoffman, Observational evidence for a boundary layer source of dayside region 1 field-aligned currents, J. Geophys. Res., 86, 5577, 1981.

Chiu, Y.T., and J.M. Cornwall, Electrostatic model of a quiet auroral arc, J. Geophys. Res., 85, 543, 1980.

Cowley, S.W.H., D.J. Southwood and M.A. Saunders, Interpretation of magnetic field perturbations in the earth's magnetopause boundary layer. Planet. Space Sci., 31, 1237, 1983.

Daly, P.W., D.J. Williams, C.T. Russell and E. Keppler, Particle signatures of magnetic flux transfer events at the magnetopause, J. Geophys Res., 86, 1628, 1981.

Eastman, T.E., E.W. Hones, Jr., S.J. Bame and J.R. Asbridge, The magnetospheric boundary layer, Site of plasma, momentum, and energy transfer from the magnetosheath into the magnetosphere, Geophys. Res. Lett., 3, 685, 1976.

Eastman, T.E., The plasma boundary layer and magnetopause layer of the earth's magnetosphere LA-7842-T, thesis, 1979.

Eastman, T.E., L.A. Frank and C.Y. Huang, The boundary layers as the primary transport regions of the earth's magnetotail, submitted to J. Geophys. Res., 1984.

Evans, D.S., Fine structure in the energy spectrum of low energy auroral electrons in Atmospheric Emissions, edited by B.M. McCormac and A. Omholt, p. 107, Van Nostrand Reinhold, New York, 1969.

Evans, D.S., Precipitating electron fluxes formed by a magnetic field-aligned potential difference, J. Geophys. Res., 79, 2853, 1974.

Evans, D.S., The characteristics of a persistent auroral arc at high latitude in the 1400 MLT sector, proceeding from NATO-conference on the Polar Cusp in Lillehammer, Norway, 7-11 May 1984.

Frank, L.A., and K.L. Ackerson, Observations of charged particle precipitation into the auroral zone, J. Geophys. Res., 76, 3612, 1971.

Frank, L.A. and D.A. Gurnett, Distributions of plasmas and electric fields over the auroral zones and polar caps, J. Geophys. Res., 76, 6829, 1971.

Haerendel, G. and G. Paschmann, Physics of the hot plasma in the magnetosphere ed. B. Hultqvist and L. Stenflo, Plenum, New York, 1975.

Haerendel, G., G. Paschmann, N. Sckopke, H. Rosenbauer, and P.C. Hedgecock, The frontside boundary layer of the magnetosphere and the problem of reconnection, J. Geophys. Res., 83, 3195, 1978.

Heikkila, W.J., Impulsive penetration and viscous interaction. Proceedings of magnetospheric boundary layer conference, Alpach, June 1979, ESA SP-148., 375, 1979.

Heikkila, W.J., Impulsive plasma transport throughout the magnetopause, Geophys. Res. Lett., 9, 159, 1982a.

Heikkila, W.J., Inductive electric field at the magnetopause, Geophys. Res.Lett., 9, 877, 1982b.

Heikkila, W.J., Magnetospheric topology of fields and currents, in Magnetospheric Currents, AGU, geophysical monograph, 28, A208, 1984.

Ijima, T., and T.A. Potemra, Large-scale characteristics of field-aligned currents associated with substorms, J. Geophys. Res., 83, 599, 1978.

Knight, S., Parallel electric fields, Planet. Space Sci., 21, 741, 1973.

Lemaire, J., Impulsive penetration of filamentary plasma elements into the magnetospheres of the earth and Jupiter, Planet. Space Sci., 25, 887, 1977.

Lemaire, J., M.J. Rycroft and M. Roth, Control of impulsive penetration of solar wind irregularities into the magnetosphere by the interplanetary magnetic field direction, Planet Space Sci., 27, 47, 1979.

Lundin, R., and I. Sandahl, Some characteristics of the parallel electric field acceleration of electrons over discrete auroral arcs as observed from two rocket flights, Symposium on European rocket research, Ajaccio, Corsica, 1978, ESA SP-135, 125, 1978.

Lundin, R. and B. Aparicio, Observations of penetrated solar wind plasma elements in the plasma mantle, Planet. Space Sci., 30, 81, 1982.

Lundin, R., B. Hultqvist, N. Pissarenko, and A. Zakharov, The plasma mantle: Composition and other characteristics observed by means of the PROGNOZ-7 satellite, Space Sci. Rev., 31, 247, 1982.

Lundin, R., B. Hultqvist, N. Pissarenko, and A. Zakharov, Composition of the hot magnetosphere, edited by R.G. Johnson, p. 307, Terra scientific publishing comp., Tokyo, 1983.

Lundin, R. and E. Dubinin, Solar wind energy transfer regions inside the dayside magnetopause. I. Evidence for magnetosheath plasma penetration, Planet. Space Sci.,32, 745, 1984.

Lundin, R., Solar wind energy transfer regions inside the dayside magnetopause, II. Evidence for an MHD-generator process, Planet.Space Sci., 32, 757, 1984.

Lundin, R. and E. Dubinin, Solar wind energy transfer regions inside the dayside magnetopause. III. Accelerated heavy ions as tracers for MHD processes in the dayside boundary layer, accepted for publication in Planet. Space Sci., 1984.

Lennartsson, W., On the role of magnetic mirroring in auroral phenomena, Astrophys. Space Sci., 51, 461, 1977.

Lennartsson, W., On the consequences of the interaction between the auroral plasma and the geomagnetic field, Planet. Space Sci., 28, 135, 1980.

Lyons, L.R., D.S. Evans and R. Lundin, An observed relation between magnetic field aligned electric fields and downward electron energy fluxes in the vicinity of the auroral forms, J. Geophys. Res., 84, 457, 1979.

Lyons, L.R., Generation of large-scale regions of auroral currents, electric potentials, and precipitation by the divergence of the convection electric field, J. Geophys. Res., 85, 17, 1980.

Lyons, L.R., Discrete aurora as the direct result of an inferred, high-altitude generating potential distribution, J. Geophys. Res., 86, 1981.

Lyons, L.R., and D.S. Evans, An association between discrete aurora and energetic particle boundaries, J. Geophys. Res., 89, 2395, 1984.

Murphree, J.S., L.L. Cogger and C.D. Anger, Characteristics of the instantaneous auroral oval in the 1200-1800 MLT sector, J. Geophys. Res., 86, 7657, 1981.

Paschmann, G., G. Haerendel, N. Sckopke, H. Rosenbauer, and P.C. Hedgecock, Plasma and magnetic field characteristics of the distant polar cusp near local noon: the entry layer, J. Geophys. Res., 81, 2883, 1976.

Paschmann, G., B.U. O. Sonnerup, I. Papamastorakis, N. Sckopke, G. Haerendel, S.J. Bame, J.S. Asbridge, J.T. Gosling, C.T. Russell, and R.C. Elphic, Plasma acceleration at the earth's magnetopause: Evidence for reconnection, Nature, 282, 243, 1979.

Paschmann, G., G. Haerendel, I. Papamastorakis, N. Sckopke, S.J. Bame, J.T. Gosling, and C.T. Russell, Plasma and magnetic field characteristics of magnetic flux transfer events, J. Geophys. Res., 87, 2159, 1981.

Robinson, R.M., D. Hardy and T. Dabbs, Gradients in the dayside boundary layer and their relation to region 1 Birkeland currents, EOS abstract, SM11A-02, AGU fall meeting, 1984.

Rostoker, G. and R. Bostrom, A mechanism for driving the gross Birkeland current configuration in the auroral oval, J. Geophys. Res., 81, 235, 1976.

Russell, C.T. and R.C. Elphic, ISEE observations of flux transfer events at the dayside magnetopause, Geophys. Res. Lett., 6, 33, 1979.

Saunders, M.A., Recent ISEE observations of the magnetopause and low latitude boundary layer: a review, J. Geophys., 52, 190, 1093.

Sckopke, N., G. Paschmann, G. Haerendel, B.U.O. Sonnerup, S.J. Bame, T.G. Forbes, E.W. Hones, and C.T. Russell, Structure of the low-latitude boundary layer, J. Geophys. Res., 86, 2099, 1981.

Sonnerup, B.U.O., Theory of the low-latitude boundary layer, J. Geophys. Res., 85, 2017, 1980.

Sonnerup, B.U.O., G. Paschmann, I. Papamastorakis, N. Sckopke, G. Haerendel, S.J. Bame, J.R. Asbridge, J.T. Gosling, and C.T. Russell, Evidence for magnetic field reconnection at the earth's magnetopause, J. Geophys. Res., 86, 10049, 1981.

Speiser, T.W. and D.J. Williams, Magnetopause modeling. Flux transfer events and magnetosheath quasi-trapped distributions, J. Geophys. Res., 87, 1982.

Stasiewicz, K., On the formation of auroral arcs, paper presented at the XXV COSPAR meeting, Graz, Austria, 1984.

Stasiewicz, K., R. Lundin and B. Hultqvist, On the interpretation of different flow vectors of different ion species in the magnetospheric boundary layer, submitted to Planet. Space Sci., 1985.

Vasyliunas, V.M., Interaction between the magnetospheric boundary layers and the ionosphere, in Magnetospheric Boundary Layers (B. Battrick ed.), pp. 387, Paris: ESA, SP-148, 1979.

Winningham, J.D., F. Yasuhara, S.-I. Akasofu, and W.J. Heikkila, The latitudinal morphology of 10-eV to 10-keV electron fluxes during magnetically quiet and disturbed times in the 2100-0300 MLT sector, J. Geophys. Res., 80, 3148, 1975.

TABLE 1

Measured and inferred source plasma parameters from PROGNOZ-7 and TIROS/N

	TIROS/N			PROGNOZ-7		
F ($erg/cm^2 s$)	V_o (V)	E_o* (eV)	n (cm^{-3})	n (cm^{-3})	$\Delta\phi$ (V)	V_l (V)
13.7	930±150	100±10	2.4	2.7±0.19	1200±100	300±100
0.95	300±100	100±10	1.0	0.89±0.06	800±100	300±100

*Based on PROGNOZ-7 electron temperature

**Referring to the 08:53 UT and 08:59 UT density enhancements.

$$\Delta\phi = \int(\underline{v}(H^+)\times\underline{B})d\underline{s}$$

$$V_l = \int(\underline{v}(O^+)\times\underline{B})d\underline{s}$$

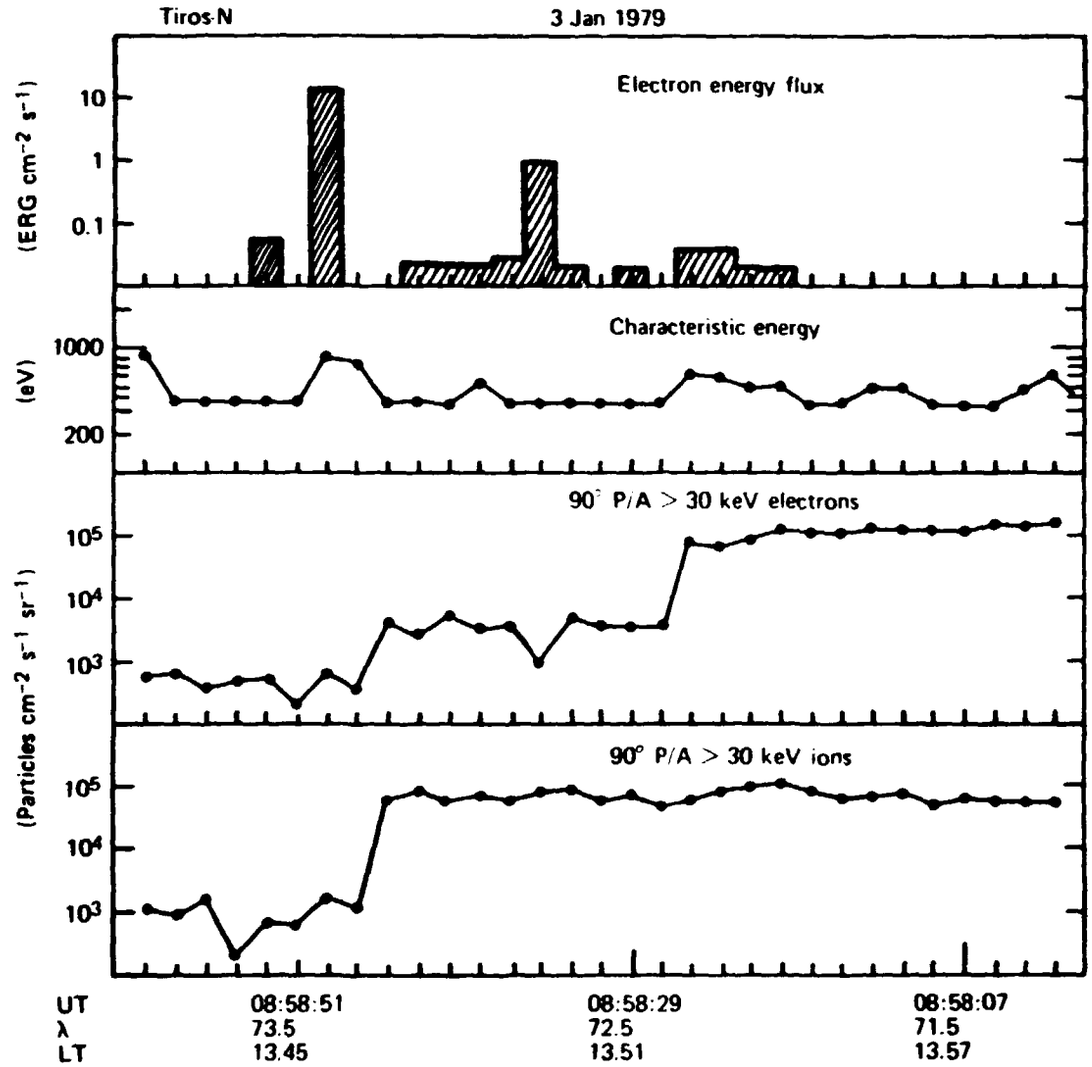

Figure 1. TIROS-N pass of the dayside auroral region at ≈13.45 MLT. The upper panel shows the precipitating electron energy flux with the highest time resolution (every ~2s). The characteristic energy is the maximum in the differential energy flux distribution. The two lowermost panels gives the flux of electrons and ions >30 keV for pitch angles of 90°.

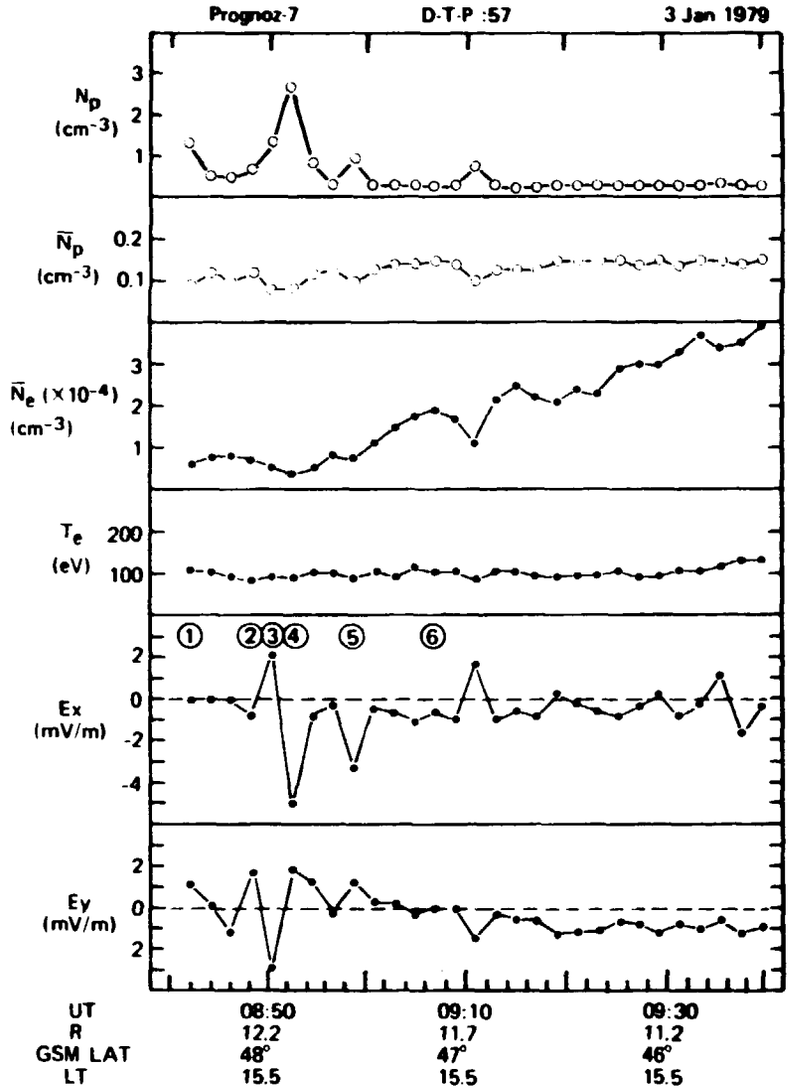

Figure 2. PROGNOZ-7 plasma data taken during an inbound pass of the dayside boundary layer at ≈48° GSM latitude and a local time of ≈15.5 (GSM). The upper panel shows the total ion density (0.03-30 keV/e). The second and third panel shows the partial ion and electron densities above 7 keV (ions) and 11 keV (electrons). The fourth panel depicts the electron temperature of the boundary layer plasma. The two lowermost panels show the x and y terms (using geocentric solar ecliptic coordinates) of the plasma $\underline{v}\times\underline{B}$ motion - given as Ex and Ey.

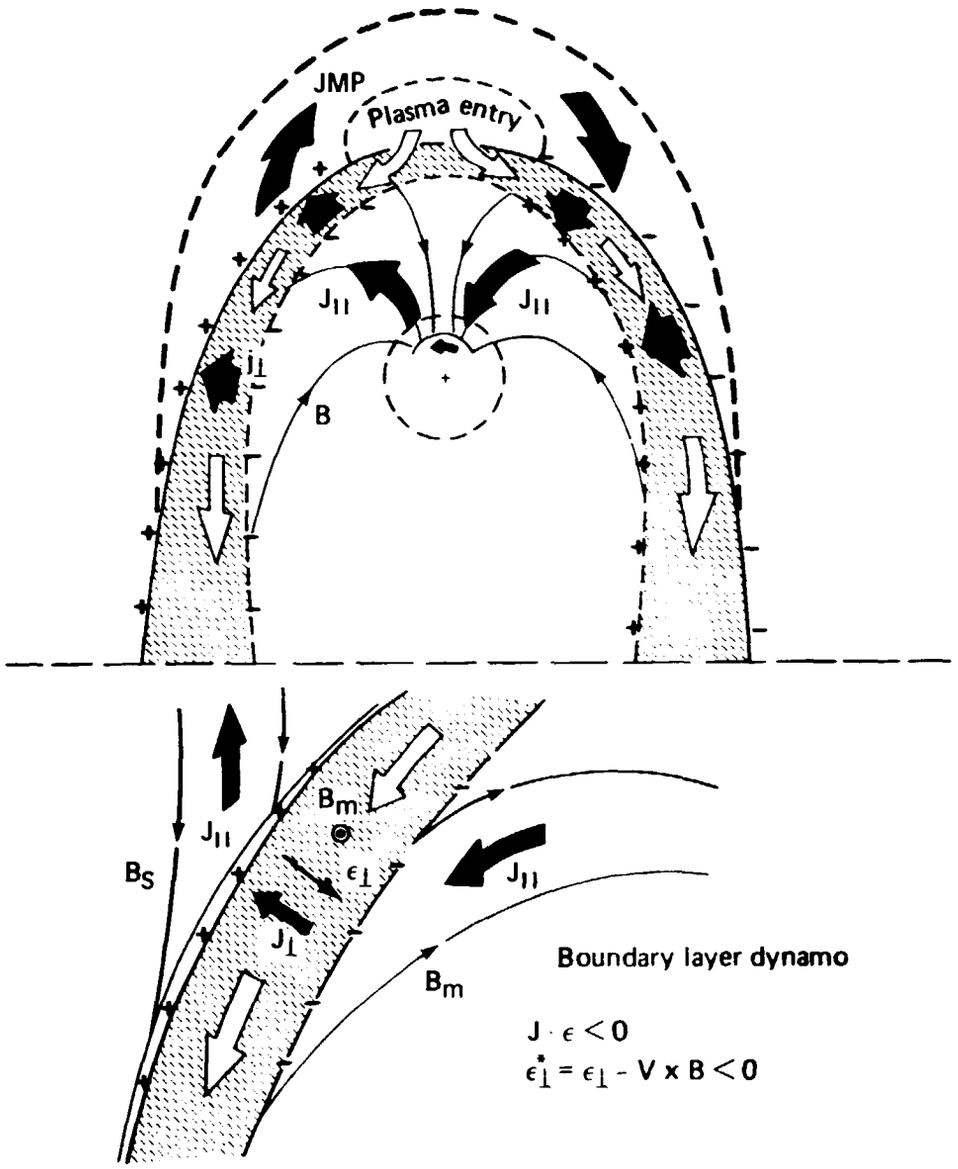

Figure 3. A model of the magnetospheric boundary layer dynamo generating currents and fields. Open arrows represents plasma flow while solid arrows represent currents. Field-aligned currents connect to the dayside auroral ionosphere (Region 1 currents) and the dayside boundary layer. Current closure is maintained by the magnetopause current (Jmp). The lower panel gives a schematic model of the boundary layer loaded dynamo polarizing the boundary layer ($\epsilon_{\perp}$) and driving currents through the ionospheric load. The replenishment of charges (loading) causes a braking action of the plasma such that $\epsilon_{\perp} \neq \underline{v} \times \underline{B}$.

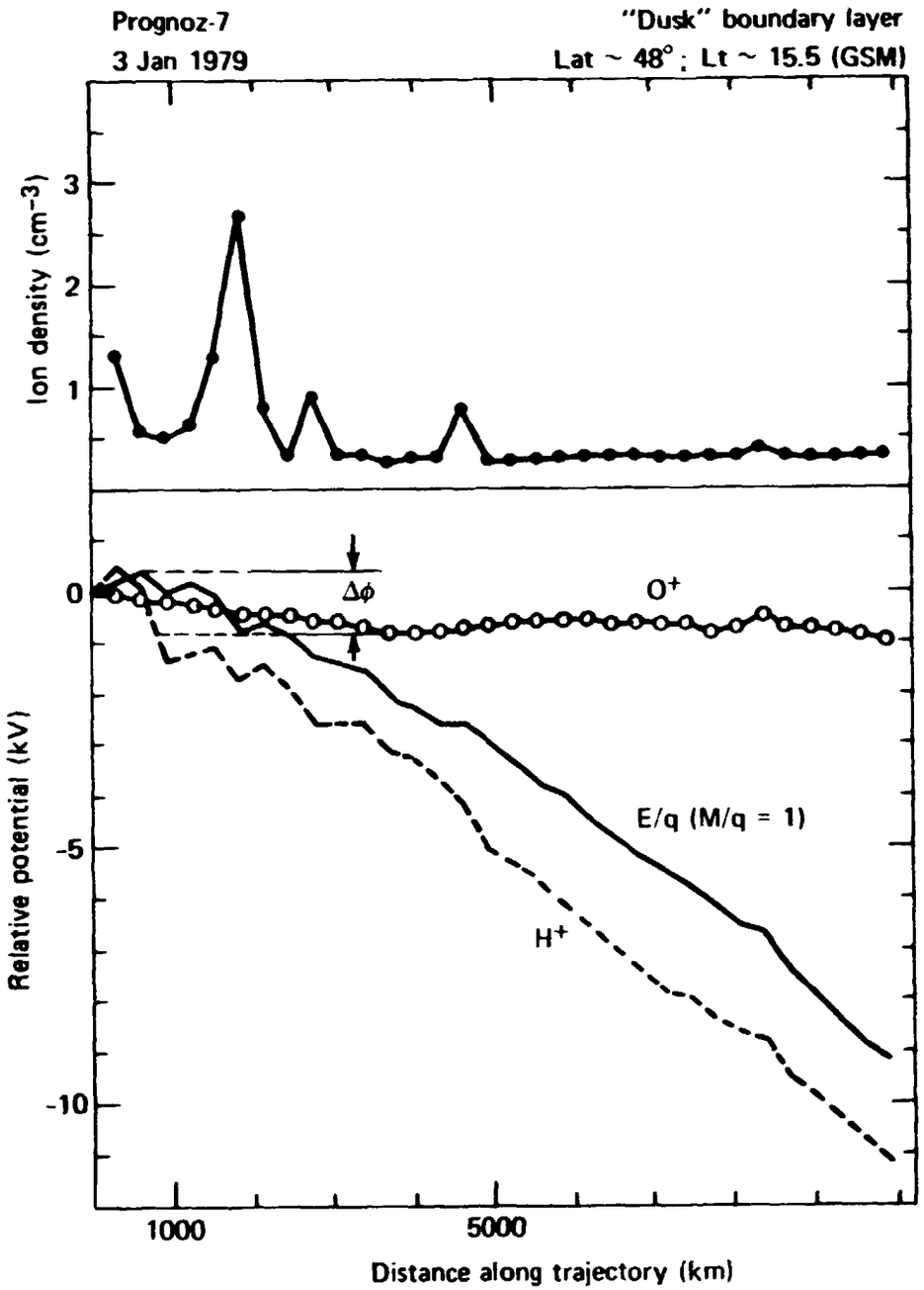

Figure 4. The relative potential deduced from the plasma $\underline{v} \times \underline{B}$ versus distance along the satellite trajectory, using the same boundary layer pass as that contained in Figure 2. The relative potential was determined for H^+ and O^+ ions as well as for the E/q ion data assuming M/q=1. The upper panel gives the measured total ion densities along the orbit. The figure also shows how the "motional EMF" was deduced from one of the direct comparison events.

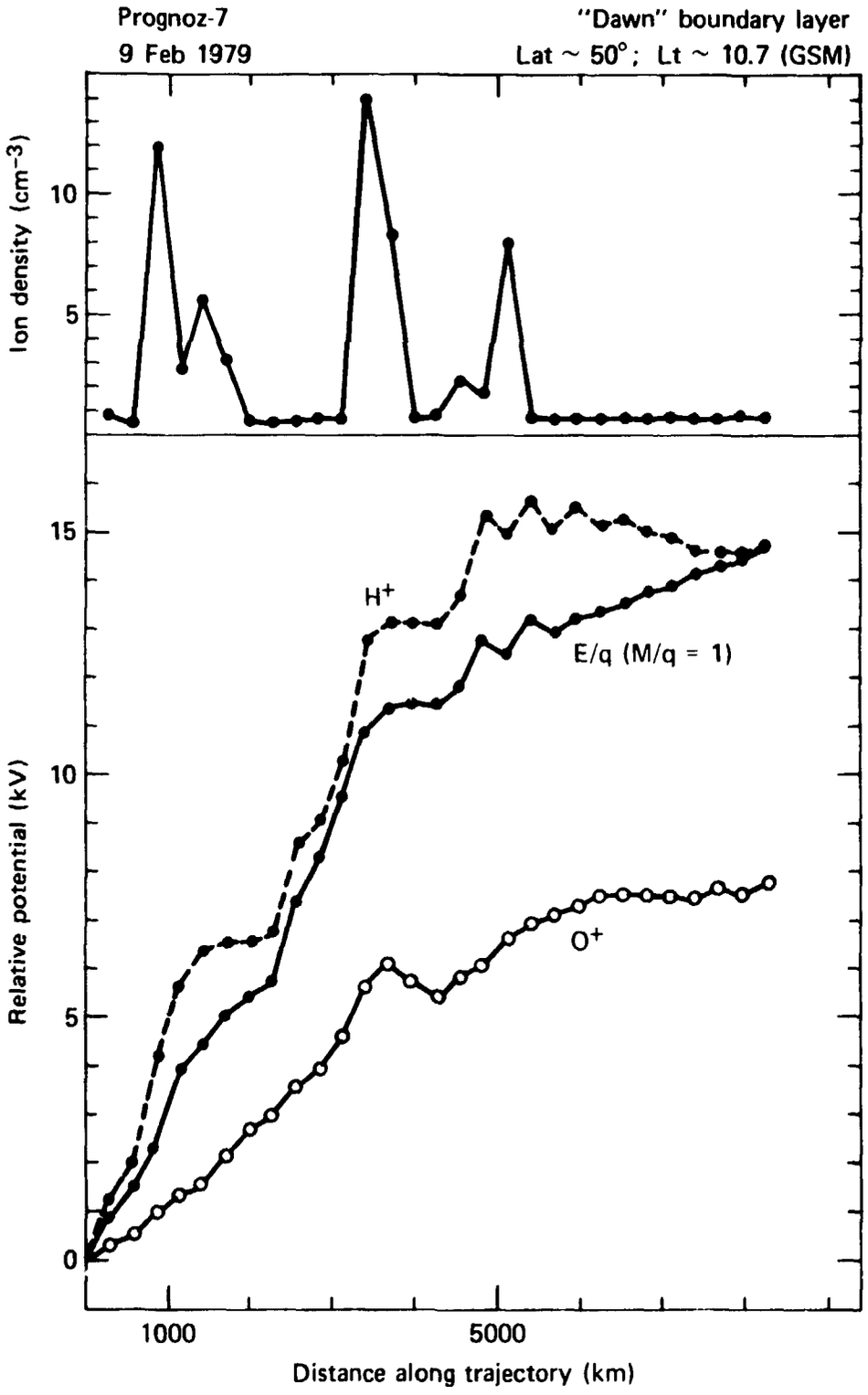

Figure 5. Same as for Figure 4, but now deduced from a "dawn" boundary layer pass with three pronounced magnetosheath injection structures in the boundary layer. The potential is here related to the time of the magnetopause crossing (≈03:19 UT). Notice the reversed polarity of this event.

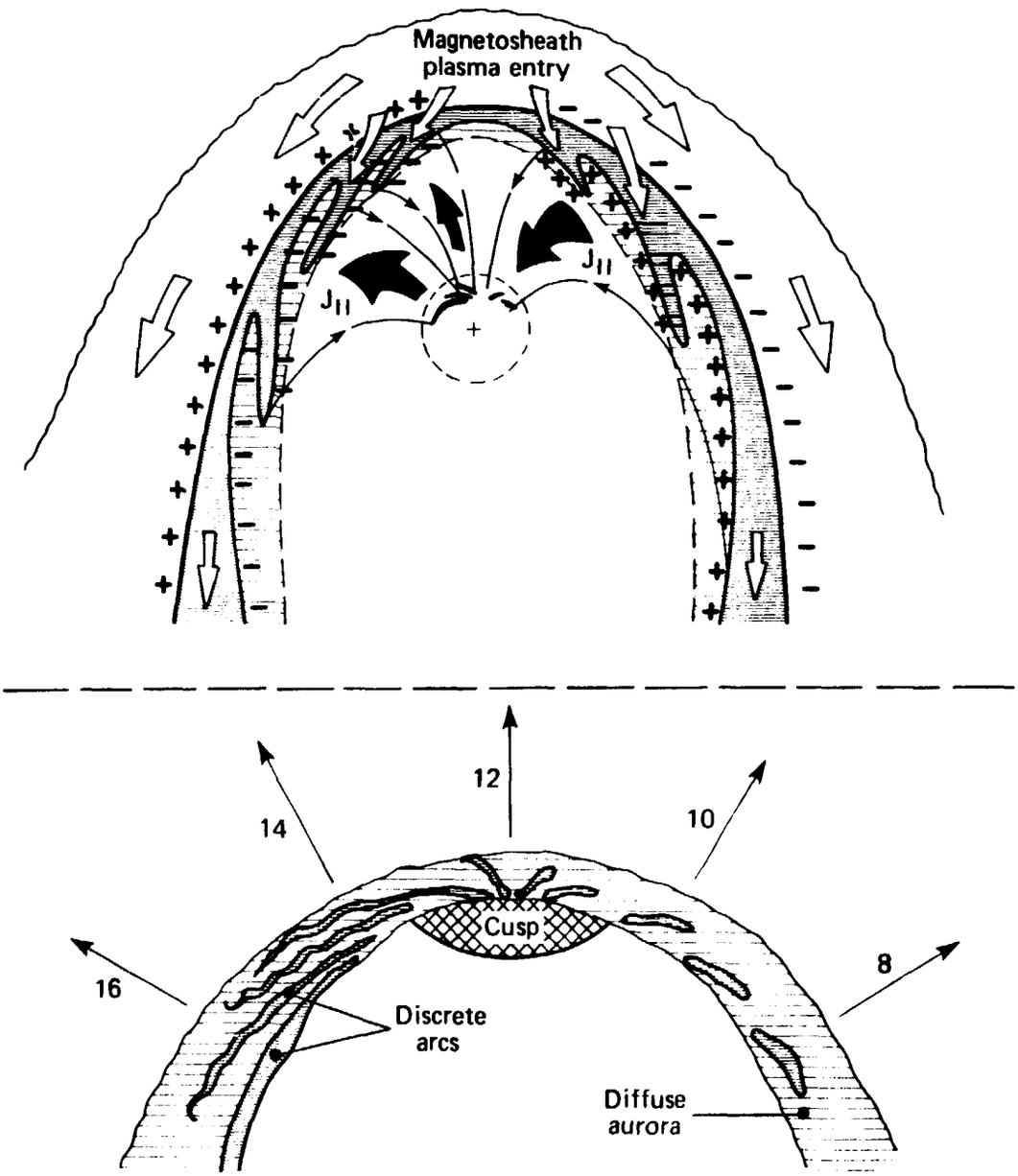

Figure 6. A model of the magnetospheric boundary layer with plasma injection filaments polarizing the boundary layer. The negative side of the injection filaments results in an upward current sheet which connects along one specific auroral arc structure. The bottom figure gives an enlarged top view of the auroral oval with discrete auroral structures embedded in diffuse aurora. The "radial" dependence with spoke-like structures which focus towards the cusp are believed to result from the injection process.

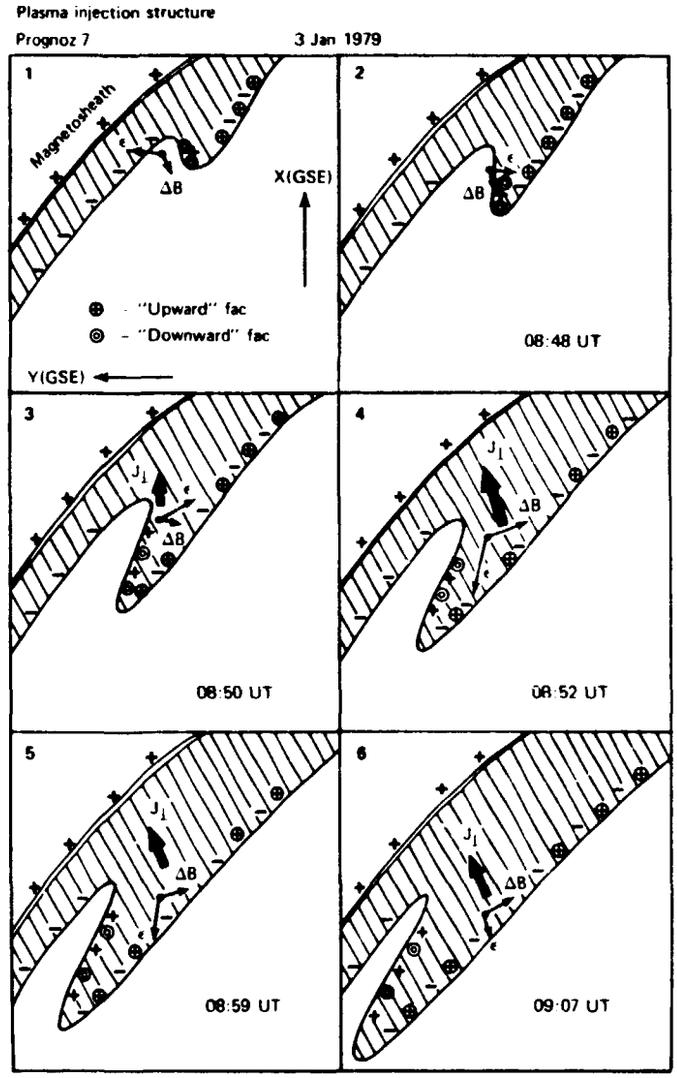

Figure 7. A temporal model illustrating the expansion of injected magnetosheath plasma in the boundary layer, based on the observed plasma characteristics from the 3 Jan 1979 boundary layer pass. The spacecraft position is given by the locus of the $\underline{\varepsilon}$ and $\underline{\Delta B}$ vectors in each panel. Each picture is a projection down to the x-y solar ecliptic plane. The $\underline{\varepsilon}$ vector was determined from the plasma $\underline{v}\times\underline{B}$ similar to that in Figure 2. The $\underline{\Delta B}$ vector was deduced from the inferred perturbation of Bx and By along the spacecraft orbit (see e.g. Lundin and Dubrinin, 1984a). From $\underline{\Delta B}$ the orientation and relative magnitude of $j_\perp$ was inferred when the satellite was inside the injection structure (panels 3-6).

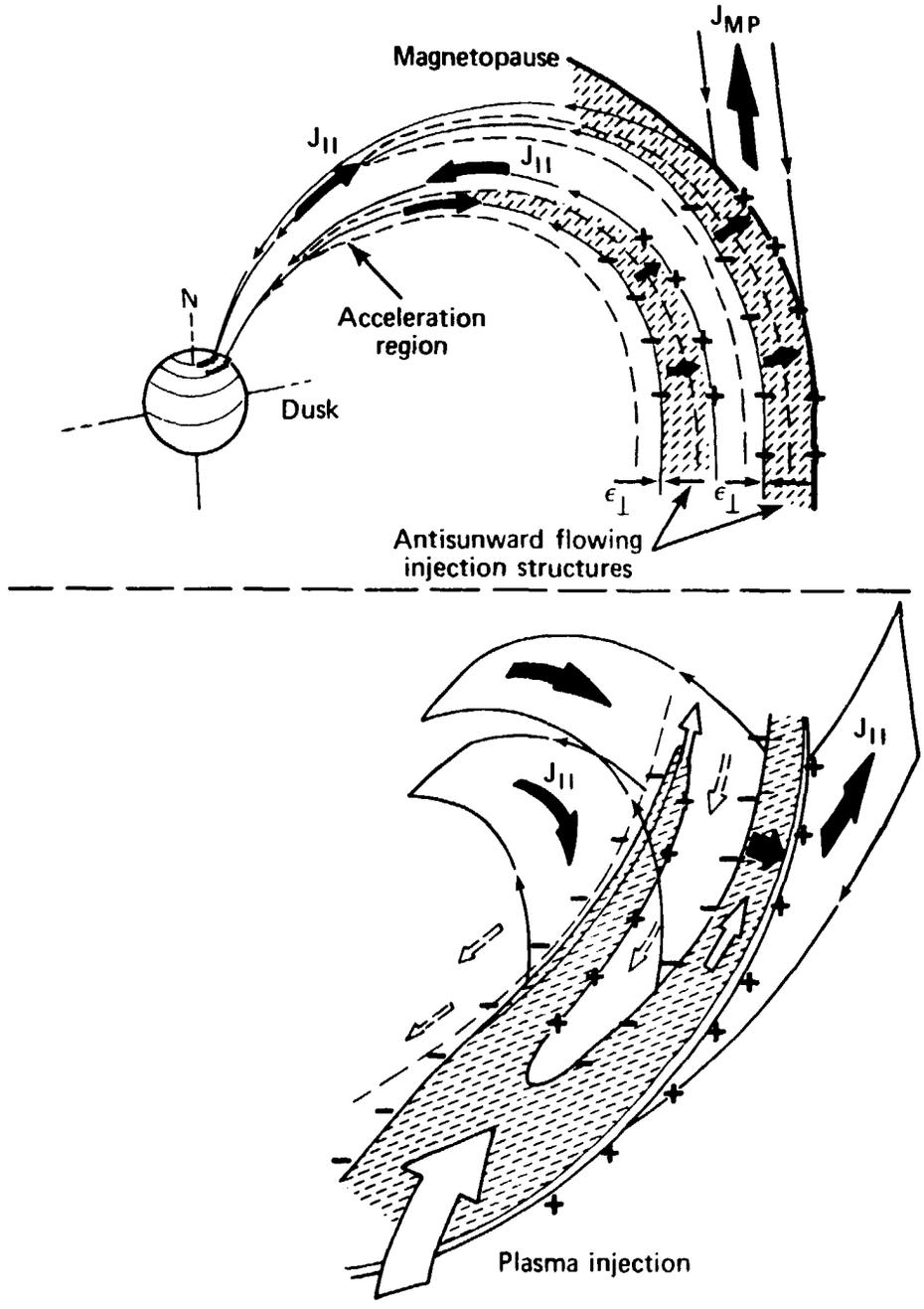

Figure 8. A model summarizing the dayside boundary layer dynamo concept with "isolated" as well as dawn-dusk coupled generator regions. The figure shows for example that the auroral acceleration regions, associated with discrete aurora, can be interpreted as an extension of the negatively charged side of the dynamo due to the lack of charge carriers (e.g. Lennartsson, 1977).